Articles

Electrocatalysis in Photochemically Activated Electropolymerized Thin Films

John A. Moss,[‡] Robert M. Leasure,[†] and Thomas J. Meyer*[,§]

Department of Chemistry, The University of North Carolina, CB#3290, Chapel Hill, North Carolina 27599-3290

Received February 25, 1999

In reductively electropolymerized thin films of poly-*cis*-$[Ru(vbpy)_2(py)_2](PF_6)_2$ ("vbpy" is 4-methyl-4′-vinyl-2,2′-bipyridine and "py" is pyridine), on glassy carbon electrodes, photochemical ligand loss with aqueous $HClO_4$ in the external solution occurs to give poly-*cis*-$[Ru(vbpy)_2(OH_2)_2](ClO_4)_2$, but the efficiency of ligand loss is greatly decreased compared to the efficiency in solution. In cyclic voltammograms of films containing the aqua complex, there is evidence for both $Ru^{III/II}$ and higher oxidation state $Ru^{IV/III}$, $Ru^{V/IV}$, and $Ru^{VI/V}$ couples. The redox chemistry of the resulting films is dictated by the film structure and can be controlled by varying the electropolymerization conditions and external solution composition. The oxidation of alcohols by these higher oxidation state couples has been investigated electrochemically.

Introduction

Polypyridyl oxo complexes of ruthenium have an extensive stoichiometric and catalytic oxidation chemistry.[1−7] They are accessible by oxidation and proton loss from aqua precursors. As an example, oxidation of *cis*-$[Ru(bpy)_2(OH_2)_2]^{2+}$ ("bpy" is 2,2′-bypyridine) provides access to Ru^{VI} by a series of stepwise reactions

$$[Ru^{II}(bpy)_2(OH_2)_2]^{2+} \underset{+e^-,H^+}{\overset{-e^-,-H^+}{\rightleftharpoons}} [Ru^{III}(bpy)_2(OH_2)(OH)]^{2+} \underset{+e^-,H^+}{\overset{-e,-H}{\rightleftharpoons}} [Ru^{IV}(bpy)_2(OH_2)(O)]^{2+} \quad (1)$$

$$[Ru^{IV}(bpy)_2(OH_2)(O)]^{2+} \underset{+e^-,H^+}{\overset{-e,-H}{\rightleftharpoons}} [Ru^{V}(bpy)_2(OH)(O)]^{2+} \underset{+e^-,H^+}{\overset{-e,-H}{\rightleftharpoons}} [Ru^{VI}(bpy)_2(O)_2]^{2+} \quad (2)$$

However, in solution, the final product, *cis*-$[Ru(bpy)_2(O)_2]^{2+}$, is unstable toward bpy ligand loss and *trans*-dioxo formation on a time scale of minutes:[8]

$$cis\text{-}[Ru^{VI}(bpy)_2(O)_2]^{2+} + 2H_2O \rightarrow trans,cis\text{-}[Ru^{VI}(bpy)(O)_2(OH)_2 + Hbpy^+ + H^+ \quad (3)$$

This instability greatly limits the use of these complexes as oxidation catalysts in solution.

Procedures have been devised for immobilizing Ru-aqua precursors in thin polymeric films on electrode surfaces by electropolymerization, creating a basis for interfacial electrocatalysis.[9,10] These procedures include oxidative electropolymerization of $Ru(pyr\text{-}bpy)_2Cl_2$[11] (pyr-bpy is 4-methyl-4′-(4-pyrrol-1-yl-ethyl)-2,2′-bipyridine) or $Ru(pyr\text{-}bpy)_2(CO_3)$[12] and reductive co-electropolymerization of $Ru(vbpy)_2(CO_3)$ (vbpy is 4-methyl-4′-vinyl-2,2′-bipyridine) and $[Ru(vbpy)_3]^{2+}$.[12] The ability of these films to act as electrocatalysts depends both on the retention of the aqua-oxo redox chemistry and on intrafilm diffusion by the reductant and its oxidized form. Soaking these films in acidic aqueous solutions leads to the formation of aqua complexes by solvolysis of the Cl^- or CO_3^{2-} ligands. The resulting films are capable of supporting oxidative electrocatalysis, but there are limitations:

(a) Incomplete or kinetically slow oxidation limits access to oxidation states past Ru^{III}.

(b) Electrocatalytic activity is lost over a period of time.

(c) Electrocatalysis does not scale with film thickness.

(d) In polypyrrole films, redox processes localized on the polymeric backbone obscure the metal-centered oxidative electrochemistry.

We are exploring ways to maximize electrocatalytic activity in these films and to incorporate catalytic oxo sites into designed film-based microstructures.

* To whom correspondence should be addressed.
† Present address: Pharmacia & Upjohn, Inc., 7000 Portage Rd., Kalamazoo, MI 49001-0199.
‡ Present address: Department of Environmental Engineering Science, California Institute of Technology, Pasadena, CA 91125.
§ Present address: Los Alamos National Laboratory, P.O. Box 1663, MS A127, Los Alamos, NM 87545.

(1) Cheng, W. C.; Yu, W. Y.; Li, C. K.; Che, C. M. *J. Org. Chem.* **1995**, *60*, 6840.
(2) Che, C. M. *Pure Appl. Chem.* **1995**, *67*, 225.
(3) Che, C. M.; Yam, V. W. W. *Adv. Inorg. Chem.* **1992**, *39*, 233.
(4) Stultz, L. K.; Binstead, R. A.; Reynolds, M. S.; Meyer, T. J. *J. Am. Chem. Soc.* **1995**, *117*, 2520.
(5) Dovletoglou, A.; Meyer, T. J. *J. Am. Chem. Soc.* **1994**, *116*, 215.
(6) Meyer, T. J. *Metal Oxo Complexes and Oxygen Activation*; Martell, A. E., Sawyerin, D. T., Eds.; Plenum Press: New York, 1988; p 33.
(7) Dobson, J. C.; Seok, W. K.; Meyer, T. J. *Inorg. Chem.* **1986**, *25*, 1514.
(8) Dobson, J. C.; Meyer, T. J. *Inorg. Chem.* **1988**, *27*, 3283.
(9) Murray, R. W. *Molecular Design of Electrode Surfaces*; John Wiley and Sons: New York, 1992; Vol. 22.
(10) Deronzier, A.; Moutet, J.-C. *Coord. Chem. Rev.* **1996**, *147*, 339.
(11) De Giovani, W. F.; Deronzier, A. *J. Chem. Soc., Chem. Commun.* **1992**, 1461.
(12) Guadalupe, A. R.; Chen, X.; Sullivan, B. P.; Meyer, T. J. *Inorg. Chem.* **1993**, *32*, 5502.

10.1021/ic990235f CCC: $19.00
Published on Web 02/23/2000

This manuscript reports a new photochemical procedure for preparing catalytically active reductively electropolymerized films, allowing control over both the film structure and the nature of the immobilized catalyst. The photochemical procedure is investigated in detail, and the electrochemical and catalytic properties of the resulting films are explored with an emphasis on the effect of the film environment on catalyst behavior. Part of this work appeared in a previous communication.[13]

Experimental Section

Materials. For electrochemical measurements, acetonitrile (Burdick and Jackson, UV grade) was deaerated by bubbling with Ar for 1 h and stored under nitrogen. Water was distilled and deionized with a Barnstead E-pure system. For synthetic procedures, all solvents and chemicals were reagent grade or better and used as received. Tetra-*N*-butylammonium hexafluorophosphate (TBAH) was prepared as described previously.[14] Tetra-*N*-butylammonium chloride (TBACl, Aldrich) was purified by a literature method.[15] All other chemicals were reagent grade and used as received. The ligand vbpy[14] and the complexes $Ru(vbpy)_2Cl_2 \cdot 2H_2O$[12] and *cis*-$[Ru(vbpy)_2(py)_2](PF_6)_2$[14] were prepared according to literature procedures.

Teflon-shrouded glassy carbon (0.071 cm^2) electrodes were constructed according to a previously described procedure[16] and polished with 1-μm diamond paste (Buehler) immediately prior to use. Tin-doped indium oxide (ITO) coated glass optically transparent electrodes (20 Ω cm^{-2} or 40 Ω cm^{-2}, Delta Technologies, Ltd.) were prepared either by soaking for 30 s in 10% HNO_3 and 2 min in distilled H_2O, CH_3OH, CH_2Cl_2, and CH_3CN or by sonicating 15 min in 1:1:5 $NH_4OH/H_2O_2/H_2O$ followed by rinsing and sonicating in distilled H_2O and CH_3CN. Electrodes prepared by the latter method were found to exhibit smaller background currents and resulted in more nearly reversible cyclic voltammetric responses. High surface area reticulated vitreous carbon electrodes (Electrosynthesis Co.) of 60 pores/in. were cleaned by soaking for 3 min in concentrated nitric acid and washing with distilled water.

Measurements. Electrochemical measurements were performed with EG&G PAR model 273 or model 263 potentiostats controlled by PC software written in-house. Rotating disk experiments were conducted with a Pine Instruments Co. rotator. The reference for all aqueous electrochemical measurements was the saturated sodium chloride calomel electrode (SSCE) without correction for junction potentials. Potentials for nonaqueous electrochemistry were acquired versus Ag/0.01 M $AgNO_3$ (0.1 M TBAH/CH_3CN) and converted to SSCE by comparing the open circuit potential between the two electrodes. Unless otherwise noted, all electrochemical measurements were carried out at room temperature. All potentials are reported versus the SSCE. Electrochemical cells were of common design. UV−vis spectra were acquired on a HP 8452A diode array spectrometer. GC-MS analysis was carried out using a Hewlett-Packard 5890 Series II gas chromatograph with a 12 m × 0.2 mm × 0.33 μm HP-1 column coupled to a Hewlett-Packard 5971A mass selective detector.

Electropolymerization. Two methods of electropolymerization were used.

Method I. Thin films of *cis*-$[Ru(vbpy)_2(py)_2](PF_6)_2$ were prepared in acetonitrile solutions, 0.5 mM in complex and 0.1 M in TBAH, by repeatedly cycling the potential of the working electrode between −0.7 and −1.7 V at 100 mV/s. Reversible, ligand-based reductions occur at −1.38 and −1.57 V for the *cis*-$[Ru(vbpy)_2(py)_2]^{2+/+}$ and *cis*-$[Ru(vbpy)_2(py)_2]^{+/0}$ couples, respectively. The film surface coverage, Γ (mol cm^{-2}), was estimated from cyclic voltammetry by integrating the area under the $Ru^{III/II}$ wave at 10 mV/s to obtain the charge passed, Q, and the relationship, $\Gamma = Q/nFA$, in which n is the number of electrons transferred, F is the Faraday constant, and A is the electrode area in cm^2.

Method II. This procedure was the same as Method I, but the working electrode was cycled 50−200 times only through the first ligand reduction from −0.70 to −1.45 V at 5 °C with a jacketed cell and circulating water bath for temperature control.

Photolysis. Broad band photolyses were carried out with a 250-W Hg lamp as described previously.[14] For photochemical reactions in films on glassy carbon disk elecrodes, light was directed through the bottom of a 25-mL scintillation vial containing 0.1 M $HClO_4$ onto the electrode surface. For films on ITO, the electrode was placed at an angle in a 1-cm cuvette and light-directed onto the electrode from the top. Solution photolyses were carried out in 1-cm quartz cuvettes with stirring and temperature control at 25 °C by using a circulating water bath. Spectra during solution and ITO photolyses were obtained in situ at right angles to the photolysis beam with an HP 8452A diode-array spectrometer. Photolyses were continued until no further change was observed in the UV−visible spectrum of the film.

Photochemical Ligand Loss Quantum Yield. The quantum yield for photochemical ligand loss was measured by photolysis of a film of poly-*cis*-$[Ru(vbpy)_2(py)_2]Cl_2$ in a 0.1 M dichloromethane solution in TBACl. The photolysis apparatus consisted of a 75-W xenon lamp powered by a high-precision constant current source coupled to a *f4* matched monochromator with 1200 lines/in. gratings. The 450-nm light from the monochromator was passed through two glass lenses onto a 1-cm glass cuvette. The electrode was positioned in the cuvette with a Teflon block, and the monochromator slits were adjusted so that the irradiation area exactly overlapped the film area. The incident light intensity, I_0^{450}, was measured by using a calibrated Si photocell.[17] The photochemical reaction was monitored by absorbance measurements in the 420−470-nm region, and the ligand loss quantum yield was calculated from the slope of absorbance change (ΔA) versus time plots at each wavelength by using eq 4:

$$\Phi_\lambda = \frac{(\text{slope})}{1000 \times I_{abs}^{450} \Delta\epsilon_\lambda} \tag{4}$$

In eq 4, Φ_λ is the calculated quantum yield at an observation wavelength λ and $\Delta\epsilon_\lambda$ is the difference in extinction coefficient in M^{-1} cm^{-1} between the reactant and photoproduct at λ. The absorbed light intensity, I_{abs}^{450}, was calculated from the absorbance of the film at 450 nm, A_{450}, as $I_{abs}^{450} = I_0^{450}(1-10^{A_{450}})$, and was assumed to remain constant throughout the measurement. This equation assumes a system of one colored photoreactant and one colored photoproduct. To ensure the validity of these assumptions, only the initial data subset was utilized in the quantum yield calculations. During this period, one set of isosbestic points was maintained.

Electrocatalytic Oxidation. Electrocatalytic oxidations of benzyl alcohol and 2-propanol were studied by cyclic voltammetry, rotated disk voltammetry, and electrolysis. For controlled-potential electrolysis of 2-propanol, a 3-mm diameter glassy carbon electrode coated with poly-*cis*-$[Ru^{II}(vbpy)_2(OH_2)_2]^{2+}$ prepared by method II was held at +1.3 V in a stirred 0.1 M $HClO_4$ solution. After the large current for initial oxidation of the film was allowed to reach a reasonable base line, an aliquot of 2-propanol was injected into the cell and the catalytic current recorded over time. A background current−time curve from electrolysis in the absence of alcohol was subtracted from the experimental curve to give plots of i_{cat} versus t.

Controlled potential electrolyses of benzyl alcohol were carried out at large surface area reticulated vitreous carbon (RVC) electrodes (electrode volume was 1 cm^3 for an ≈1000-cm^2 surface area) coated with poly-*cis*-$[Ru(vbpy)_2(OH_2)_2]^{2+}$. The solutions were 0.1 M in benzyl alcohol and 0.1 M in $HClO_4$, and the electrode potential was held at +1.3 V. After 5 h the electrolysis solution (3 mL) was loaded onto a

(13) Leasure, R. M.; Moss, J. A.; Meyer, T. J. *Inorg. Chem.* **1994**, *33*, 1247.
(14) Leasure, R. M.; Ou, W.; Moss, J. A.; Linton, R. W.; Meyer, T. J. *Chem. Mater.* **1996**, *8*, 264.
(15) Perrin, D. D.; Armarego, W. L. F. *Purification of Laboratory Chemicals*, 3rd ed.; Pergamon Press: Oxford, 1992.
(16) Brandt, E. S. A Study of Surfaces Using ESCA and Electrochemistry. Ph.D. Thesis, University of North Carolina, Chapel Hill, NC, 1978.

(17) For light intensity measurements, a single-crystal silicon photocell was calibrated with a known standard detector (UDT Instruments, model S370 optometer). The calibration was checked before and after quantum yield measurements with chemical actinometry using Reinecke's salt.

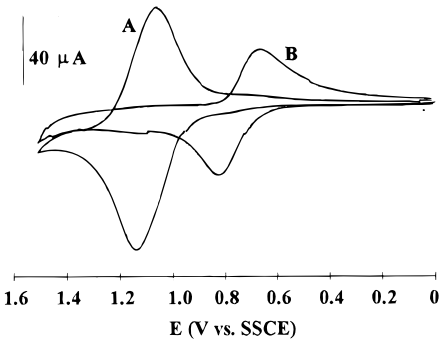

Figure 1. Cyclic voltammograms of (A) poly-*cis*-$[Ru(vbpy)_2(py)_2](PF_6)_2$, $\Gamma = 5.0 \times 10^{-9}$ mol cm^{-2} on a 3-mm glassy carbon electrode in 0.1 M TBAH/CH_3CN and (B) poly-*cis*-$[Ru(vbpy)_2(OH_2)_2](ClO_4)_2$ in 0.1 M $HClO_4/H_2O$ formed during 15 min of photolysis in 0.1 M $HClO_4$.

10-cm SP Sephadex C-25 cation-exchange column and eluted with water to remove the electrolyte. The aqueous volume was reduced to ~20 mL at 25 °C and the oxidation products were extracted into CH_2Cl_2 and analyzed by GC-MS. The retention times and mass spectra of the product peaks were compared to known standards for benzaldehyde and benzyl alcohol.

Results

Electropolymerization. In thin films of poly-*cis*-$[Ru(vbpy)_2(py)_2](PF_6)_2$ prepared by method I on glassy carbon or ITO electrodes, reversible, ligand-based reductions appear at −1.38 and −1.57 V for the poly-*cis*-$[Ru(vbpy)_2(py)_2]^{2+/+}$ and poly-*cis*-$[Ru(vbpy)_2(py)_2]^{+/0}$ couples, respectively. Films with surface coverages in the range from 5×10^{-10} to 5×10^{-8} mol cm^{-2} were prepared by varying the number of reductive cycles from 4 to 60. Polymerization by method II results in slower growth, with 200 cycles yielding a surface coverage of $\sim 2 \times 10^{-9}$ mol cm^{-2}. Films prepared by either method exhibit nearly identical electrochemical responses in 0.1 M CH_3CN solutions in TBAH. The $Ru^{III/II}$ couple appears at +1.22 V for method I and at +1.21 V for method II.

Photochemical Ligand Loss. Quantum yields for successive photochemical pyridine loss from *cis*-$[Ru(bpy)_2(py)_2]^{2+}$ in H_2O to give *cis*-$[Ru(bpy)_2(py)(OH_2)]^{2+}$ and then *cis*-$[Ru(bpy)_2(OH_2)_2]^{2+}$ are 0.26 and <0.07, respectively.[18,19] Photolysis of poly-*cis*-$[Ru(vbpy)_2(py)_2](PF_6)_2$ [$E_{1/2}(Ru^{III/II}) = +1.22$ V] on a glassy carbon electrode in 0.1 M $HClO_4$ (Figure 1) gives poly-*cis*-$[Ru(vbpy)_2(OH_2)_2]^{2+}$ [$E_{1/2}(Ru^{III/II}) = +0.71$ V]. There is no evidence for poly-*cis*-$[Ru(vbpy)_2(py)(OH_2)]^{2+}$ [$E_{1/2} = +0.79$ V] as an intermediate.

Photosubstitution of pyridine by Cl^- in poly-*cis*-$[Ru(vbpy)_2(py)_2](PF_6)_2$ (on ITO, $\Gamma = 1.0 \times 10^{-8}$ mol cm^{-2}),[20] eq 5, was studied in 0.1 M CH_2Cl_2 in TBACl.

$$\text{poly-}cis\text{-}[Ru(vbpy)_2(py)_2]^{2+} + Cl^- \xrightarrow{h\nu} \text{poly-}cis\text{-}[Ru(vbpy)_2(py)(Cl)]^+ + py \quad (5a)$$

$$\text{poly-}cis\text{-}[Ru(vbpy)_2(py)(Cl)]^+ + Cl^- \xrightarrow{h\nu} \text{poly-}cis\text{-}Ru(vbpy)_2Cl_2 + py \quad (5b)$$

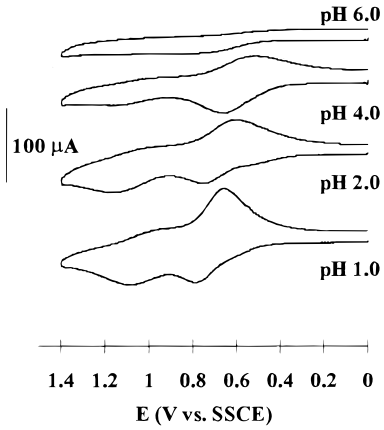

Figure 2. Cyclic voltammograms of poly-*cis*-$[Ru(vbpy)_2(OH_2)_2](ClO_4)_2$ (by method II) on a 3-mm diameter glassy carbon electrode in $HClO_4/NaClO_4$ ($\mu = 0.1$ M) at 10 mV/s.

Irradiation at 450 nm ($I_0^{450} = 7.3 \times 10^{-10}$ einstein s^{-1}) exactly overlapped the film area so that the entire photolysis beam was incident on the film and the entire film area was irradiated, allowing calculation of the absorbed intensity as $I_{abs}^{450} = 1.1 \times 10^{-10}$ einstein s^{-1} using the absorbance of the film as described in the Experimental Section. Spectral changes observed during photolysis are consistent with eq 5, exhibiting a shift in λ_{max} from 464 nm (poly-*cis*-$[Ru(vbpy)_2(py)_2]^{2+}$) to 510 nm (poly-*cis*-$[Ru(vbpy)_2(py)Cl]^+$) with an isosbestic point at 482 nm during the first hour followed by a further shift to 560 nm (poly-*cis*-$Ru(vbpy)_2Cl_2$) at longer photolysis times. From the absorbance spectra, plots of ΔA ($\Delta A = A_t - A_0$ where A_t is the absorbance at time t and A_0 is the initial absorbance) versus t were made for observation wavelengths from 420 to 470 nm. The quantum yield, Φ_λ, for loss of py, calculated from the slopes of these lines by using eq 4 and solution molar extinction coefficients for *cis*-$[Ru(dmb)_2(py)_2](PF_6)_2$ (dmb is 4,4′-dimethyl-2,2′-bipyridine), *cis*-$[Ru(dmb)_2(py)Cl](PF_6)$, and *cis*-$Ru(dmb)_2Cl_2$.[14,21] Φ_λ was found to be 0.0042 ± 0.0006, independent of monitoring wavelength.

Redox Properties. In solution, *cis*-$[Ru(bpy)_2(OH_2)_2]^{2+}$ undergoes the series of pH-dependent oxidations in eq 2.[8] In the films, the $Ru^{III/II}$ couple appears, but oxidation to the higher oxidation states is kinetically hindered. Films prepared by method I show little or no electrochemical response for couples past $Ru^{III/II}$ on the cyclic voltammetry time scale. Higher oxidation state couples do appear in films prepared by method II, but electroactivity decreases with successive scans or increasing pH (Figure 2). What appear to be overlapping $Ru^{III/II}$ and $Ru^{IV/III}$ waves occur at $E_{1/2} = +0.71$ V at pH 1 with a higher oxidation state couple at $E_{1/2} \sim +1.05$ V. For the solution couples of *cis*-$[Ru(bpy)_2(OH_2)_2]^{2+}$ at this pH, $E_{1/2}(Ru^{III/II}) = +0.66$ V, $E_{1/2}(Ru^{IV/III}) = +0.86$ V, $E_{1/2}(Ru^{V/IV}) = +1.03$ V, and $E_{1/2}(Ru^{VI/V}) = +1.25$ V.[8] These waves are pH-dependent, but less so than the analogous solution couples. For the wave at lower potential, $E_{1/2}$ varies from +0.73 V at pH 0 to +0.65 at pH 4.

After repeated cycles, the peak current for the higher oxidation state couple decreases markedly, less so for the $Ru^{III/II}$ couple. Soaking the film for several hours in 0.1 M $HClO_4$ is sufficient to recover a significant fraction of the original electrochemical response for films prepared by method I. For films prepared by

(18) Durham, B.; Walsh, J. L.; Carter, C. L.; Meyer, T. J. *Inorg. Chem.* **1980**, *19*, 860.
(19) Pinnick, D. V.; Durham, B. *Inorg. Chem.* **1984**, *23*, 1440.
(20) The surface coverage, Γ (mol cm^{-2}), was calculated from the absorbance at 464 nm by using the relationship $A = 1000\epsilon\Gamma$ with $\epsilon = 8000$ M^{-1} cm^{-1}.
(21) Leasure, R. M. Fabrication and Characterization of Microstructures in Metallopolymeric Films on Electrode Surfaces. Ph.D. Thesis, University of North Carolina, Chapel Hill, NC, 1995.

Table 1. Oxidation of Alcohols at Poly-*cis*-$[Ru(vbpy)_2(OH_2)_2]^{2+}$

		electrolysis[c]	
alcohol[a]	CV i_{cat} (μA)[b]	t (s)	$10^3 \times Q$ (C)
methanol[d]		430	0.08
ethanol	21.2	906	2.5
2-propanol	24.2	866	3.5
1-butanol	18.3	945	5.0
benzyl alcohol	36.6	866	6.4

[a] Oxidation by poly-*cis*-$[Ru(vbpy)_2(OH_2)_2]^{2+}$-coated 3-mm glassy carbon electrodes ($\Gamma = 5.0 \times 10^{-9}$ mol cm^{-2}) in 0.1 M stirred solutions in alcohol and $HClO_4$. [b] Peak current for the region $E > +1.0$ V in cyclic voltammograms at 50 mV/s in 0.1 M TBAH/CH_3CN. [c] Controlled potential electrolysis at $E_{app} = +1.25$ V. Q is the charge passed in coulombs (C) during an electrolysis time, t. [d] For methanol no catalytic wave was observed in the CV. Upon electrolysis, a rapidly decaying current was observed for the initial oxidation of the Ru catalyst with no evidence for methanol oxidation.

either method, soaking the films in CH_2Cl_2 (2−4 h) followed by soaking in 0.1 M $HClO_4$ (0.5−1 h) results in nearly complete recovery of the initial electroactivity.

UV−visible spectra following oxidation of poly-*cis*-$[Ru(vbpy)_2(OH_2)_2](PF_6)_2$ on ITO ($\Gamma = 7 \times 10^{-9}$ mol cm^{-2}) by method I were obtained at 100-mV potential steps from 0 to 1.3 V. Oxidation of Ru^{II} to Ru^{III} at +0.97 V results in the loss of the metal-to-ligand charge transfer (MLCT) band at 480 nm. By +1.30 V, where Ru^{VI} should be the dominant form, a new absorption appears at 315 nm.

Oxidation Catalysis. Catalytic oxidation of a series of alcohols by poly-*cis*-$[Ru(vbpy)_2(OH_2)_2](ClO_4)_2$ on a 3-mm diameter glassy carbon electrode in 0.1 M $HClO_4$ was investigated by cyclic voltammetry and potential step electrolysis. Catalytic waves for oxidation of the alcohol occurred at onset potentials corresponding to the $Ru^{V/IV}$ couple in solution. Oxidation by controlled potential electrolysis at +1.25 V was also investigated with the area under current−time plots used to calculate the total charge passed. Results are summarized in Table 1.

Oxidation of benzyl alcohol was studied at large surface area RVC electrodes coated first with poly-*cis*-$[Ru(vbpy)_2(py)_2](PF_6)_2$ (method I) and converted into poly-*cis*-$[Ru(vbpy)_2(OH_2)_2](ClO_4)_2$ by photolysis for 1 h in aqueous 0.1 M $HClO_4$. Polymerization and photolysis on a glassy carbon disk were conducted in parallel and followed by cyclic voltammetry to monitor the reactions on RVC. In a typical experiment, the potential of the RVC electrode was stepped to +1.3 V in stirred 0.1 M $HClO_4$ in benzyl alcohol. The initial current of ~27 mA decreased to ~4 mA after 2 h. After 5 h of electrolysis, 51.8 C had passed. Extraction of the organic products into dichloromethane and analysis by GC-MS identified benzaldehyde as the oxidation product.

Oxidation kinetics were investigated by rotated disk linear sweep voltammetry at a 3-mm diameter glassy carbon electrode. In Figure 3 are shown voltammograms at bare and film-coated electrodes. Characteristic oxidative waves for the diaqua film are observed at +0.74 and +0.88 V in the absence of benzyl alcohol. In the presence of benzyl alcohol, the onset of catalytic oxidation is observed at +0.75 V with features at +0.86 and +1.03 V, the potentials for the $Ru^{IV/III}$ and $Ru^{V/IV}$ couples in solution. The catalytic current was independent of rotation rate from 200 to 2500 rpm.

Catalytic oxidation of 2-propanol was investigated by potential step-injection electrolysis experiments at glassy carbon electrodes. The electrode potential was stepped to +1.25 V in 0.1 M $HClO_4$, and an aliquot of 2-propanol was injected after

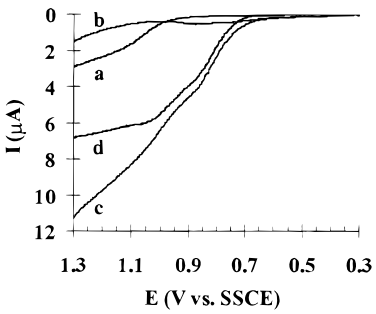

Figure 3. Rotated disk voltammograms (2000 rpm, potential scan from +0.30 to +1.30 V at 1 mV/s) (a) at a bare glassy carbon disk (0.071 cm^2) in 0.1 M $HClO_4$ with 0.1 M $C_6H_5CH_2OH$, (b) at a glassy carbon disk coated with poly-*cis*-$[Ru(vbpy)_2(OH_2)_2](ClO_4)_2$ ($\Gamma = 1.3 \times 10^{-8}$ mol cm^{-2}) in 0.1 M $HClO_4$, (c) as in (b) with 0.1 M $C_6H_5CH_2OH$, and (d) curves (a) and (b) subtracted from (c) for background correction.

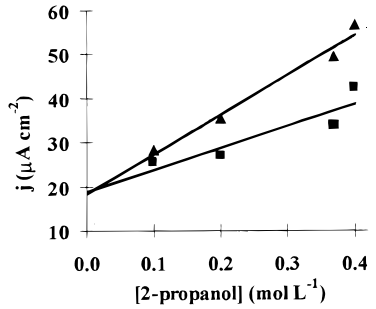

Figure 4. Variation of catalytic current density with [2-propanol] in 0.1 M $HClO_4$, 90 s (▲) and 600 s (■) after injection of 2-propanol. Potential step to +1.3 V, $\Gamma = 1.3 \times 10^{-9}$ mol cm^{-2}; see text for details.

the currents due to double-layer formation and initial film oxidation had decreased to a reasonably flat base line. The steady-state catalytic current, i_{cat}, calculated as the difference between the background and electrolysis currents, was relatively constant and increased linearly with 2-propanol concentration (Figure 4).

The role of film thickness was investigated in films from $\Gamma = 2 \times 10^{-10}$ mol cm^{-2} to $\Gamma = 3 \times 10^{-8}$ mol cm^{-2} by comparing plots of i_{cat} versus Γ and of (i_{cat}/Γ) versus Γ. As shown by the data in the Supporting Information, Figure S1, i_{cat} increases roughly linearly with log Γ, but i_{cat}/Γ decreases dramatically with log Γ. i_{cat}/Γ decreases from 4700 A cm^2 mol^{-1} at $\Gamma = 1.9 \times 10^{-10}$ mol cm^{-2} to 75 A cm^2 mol^{-1} at $\Gamma = 3.4 \times 10^{-8}$ mol cm^{-2}.

Discussion

Photochemical Ligand Loss. In previous studies, films were prepared containing aqua precursors to Ru-oxo catalysts by solvolysis of chloride or carbonate ligands,[11,12] or by direct oxidative polymerization of a pyrrole-containing aqua complex.[22] In the photochemical procedure used here, diaqua sites are created quantitatively by photochemical ligand loss. There is a well-established ligand-loss photochemistry for related pyridyl complexes in solution,[18,19] and it was applied earlier to the formation of microstructures in films of poly-*cis*-$[Ru(tmb)_2(vpy)_2](PF_6)_2$[23] and poly-*cis*-$[Ru(vbpy)_2(py)_2](PF_6)_2$.[13,21]

On the basis of electrochemical monitoring, photolysis of poly-*cis*-$[Ru(vbpy)_2(py)_2](ClO_4)_2$ appears not to occur with poly-*cis*-$[Ru(vbpy)_2(py)(OH_2)](ClO_4)_2$ as a discrete intermediate,

(22) Collomb-Dunand-Sauthier, M.-N.; Deronzier, A.; Navarro, M. *J. Chem. Soc., Chem. Commun.* **1996**, 2165.
(23) Gould, S.; O'Toole, T. R.; Meyer, T. J. *J. Am. Chem. Soc.* **1990**, *112*, 9490.

suggesting that $\Phi_2 > \Phi_1$ for stepwise ligand loss. However, $E_{1/2}$ values for the $Ru^{III/II}$ couples of *cis*-$[Ru(vbpy)_2(py)(OH_2)](ClO_4)_2$ and *cis*-$[Ru(vbpy)_2(OH_2)_2](ClO_4)_2$ in solution are +0.79 and +0.71 V at pH 1, and in a film, separate waves for the two products may not have been discernible in the cyclic voltammograms.

Additionally, photolysis of poly-*cis*-$[Ru(vbpy)_2(py)_2]^{2+}$ with added Cl^- is stepwise, but the integrated peak areas for the poly-*cis*-$[Ru(vbpy)_2(py)Cl]^+$ intermediates are ~40% less than those for the initial bis−py complex or the poly-*cis*-$Ru(vbpy)_2Cl_2$ product.[14,21] Photolysis initially produces isolated py−Cl sites in a py−py environment. They are not oxidized until oxidation at a neighboring py−py site occurs at +1.21 V. This decreases the contribution to the current from the py−Cl sites. The same phenomenon may occur in the aqueous photolysis of poly-*cis*-$[Ru(vbpy)_2(py)_2]^{2+}$, obscuring the electrochemical observation of poly-*cis*-$[Ru(vbpy)_2(py)(OH_2)]$ as a discrete intermediate.

The photochemical quantum yield measurement is more difficult for electropolymerized films compared to solution, and our method relies on several assumptions. First, the thin film does not allow complete absorption of the incident light, so the absorbed light intensity must be calculated from the incident intensity and the film absorption at 450 nm. The film absorption at 450 nm changes during photolysis as poly-*cis*-$[Ru(vbpy)_2(py)Cl]^+$ also absorbs at 450 nm. This change may be neglected, however, because only the first part of the reaction was followed and the fraction of the light absorbed by poly-cis-$[Ru(vbpy)_2(py)_2]^{2+}$ changes by less than 3% during the photolysis experiment. Second, extinction coefficient values for the quantum yield calculation were obtained from solution measurements of *cis*-$[Ru(dmb)_2(py)_2]^{2+}$. The dimethylbipyridine complexes more closely resemble the film complexes than *cis*-$[Ru(vbpy)_2(py)_2]^{2+}$ as the electropolymerization results in a cross-linked polyethylene polymer backbone with pendant bipyridine complexes exhibiting a ligand electronic structure closely resembling that of dmb.

Compared to *cis*-$[Ru(bpy)_2(py)_2]Cl_2$ in CH_2Cl_2 solution, the quantum yield for photochemical substitution in poly-*cis*-$[Ru(bpy)_2(py)_2]Cl_2$ is decreased by a factor of ~50. The photolability of the monodentate ligands in these complexes has been attributed to the presence of low-lying dd states of electronic configuration $d\pi^5 d\sigma^{*1}$ [19,24] with the dd states populated by thermal activation and surface crossing following MLCT excitation.[24−28] Once formed in solution, these metal-centered states undergo ligand loss or rapid nonradiative decay.

In rigid media including solvent glasses, polyethylene oxide, cellulose acetate, zeolites, cation-exchange resins, and Vycor glass, ligand-loss photochemistry is greatly inhibited.[29−34] In a SiO_2 sol−gel, even *cis*-$[Ru(bpy)_2(py)_2]^{2+}$, which is highly photosensitive in solution, is relatively photoinert.[35]

Given these observations, the inhibition to ligand-loss photochemistry in the electropolymerized films is not surprising. Even so, complete photoconversion of poly-*cis*-$[Ru(vbpy)_2(py)_2]Cl_2$ to poly-*cis*-$Ru(vbpy)_2Cl_2$ in films of $\Gamma = 10^{-10}-10^{-7}$ mol cm^{-2} occurs in less than 15 min with broad-band, visible irradiation from a 250-W Hg lamp. Photosubstitution also occurs in dry films showing that ion-paired Cl^- is capable of undergoing substitution, even in the absence of solvent.

Redox Properties. Previous investigations of catalysts immobilized in electropolymerized thin films have not addressed the link between film structure and redox and catalytic properties. The two major contributors to film structure variation in electropolymerized vinylbipyridine complexes are electropolymerization conditions and solvent. Initially, these effects have served to obscure the redox properties and catalytic activity of these films, but they may also allow control of these characteristics by dictating internal film structure.

The differences in redox properties between films prepared by method I and method II indicate that the film structure plays a dominant role in dictating the reactivity of the immobilized metal complex. A dramatic decrease in the electropolymerization rate is observed for method II films compared to that of method I films. Films prepared by method II are less highly cross-linked and more permeable to solvent, protons, and counterions than films prepared by method I. When polymerization is carried out by cycling through only one vbpy reduction, each reduced complex contains only one vbpy radical, decreasing the polymerization rate and number of attachment points of each complex to the vbpy backbone. Also, the singly reduced complex has a charge of +1 while doubly reduced complexes are neutral, leading to an electrostatic repulsion between *cis*-$[Ru(vbpy^{-\bullet})(vbpy)(py)_2]^+$ and unreduced *cis*-$[Ru(vbpy)_2(py)_2]^{2+}$ and decreasing the overall reaction rate.

Evidence for the role of film structure on redox behavior is quite evident following photochemical conversion from poly-*cis*-$[Ru(vbpy)_2(py)_2]^{2+}$ to poly-*cis*-$[Ru(vbpy)_2(OH_2)_2]^{2+}$. In films prepared by method II, there is less cross-linking and, presumably, a more open film structure. In highly cross-linked films prepared by method I, no waves for oxidation of Ru^{III} to higher oxidation states are observed as they are in solution. Higher oxidation states are observable in cyclic voltammograms of films prepared by method II, but assignment of individual one-electron, one-proton couples is not possible with the broad waves observed. Spectroelectrochemical measurement of absorption spectra of films following oxidation was carried out, and the spectral changes between films in oxidation states from Ru^{III} to Ru^{VI} were too small to be observed. As discussed elsewhere in this report, however, the presence of complexes of Ru^{IV} and possibly Ru^{V} and Ru^{VI} is confirmed by the catalytic activity of the films toward alcohol oxidation. For the related complex *cis*-$[Ru(bpy)(py)(OH_2)]^{2+}$ in solution, catalytic activity toward benzyl alcohol oxidation is observed for Ru^{IV}, but not for Ru^{III}. With these limitations in mind, the redox behavior of the aqua films will be further discussed assuming that the higher oxidation states (from Ru^{IV} to Ru^{VI}) observed in solution are obtained in the films, but on a slower time scale.

A remarkable property of these films is their ability to stabilize Ru^{VI}, presumably as poly-*cis*-$[Ru(vbpy)_2(O)_2]^{2+}$. In solution, *cis*-$[Ru(bpy)_2(O)_2]^{2+}$ undergoes decomposition through bpy ligand loss in a matter of minutes (eq 3).[8] The films are

(24) Durham, B.; Caspar, J. V.; Nagle, J. K.; Meyer, T. J. *J. Am. Chem. Soc.* **1982**, *104*, 4803.
(25) Van Houten, J.; Watts, R. J. *J. Am. Chem. Soc.* **1976**, *98*, 4853.
(26) Caspar, J. V.; Meyer, T. J. *J. Am. Chem. Soc.* **1983**, *105*, 5583.
(27) Hager, G. D.; Crosby, G. A. *J. Am. Chem. Soc.* **1975**, *97*, 7031.
(28) Barigelletti, F.; De Cola, L.; Juris, A. *Gazz. Chim. Ital.* **1990**, *120*, 545.
(29) Campagna, S.; Bartolotta, A.; Di Marco, G. *Chem. Phys. Lett.* **1993**, *206*, 30.
(30) Masschelein, A.; Kirsch-De Mesmaeker, A.; Willsher, C. J.; Wilkinson, F. *J. Chem. Soc., Faraday Trans.* **1991**, *87*, 259.
(31) Maruszewski, K.; Kincaid, J. R. *Inorg. Chem.* **1995**, *34*, 2002.
(32) Maruszewski, K.; Strommen, D. P.; Kincaid, J. R. *J. Am. Chem. Soc.* **1993**, *115*, 8345.
(33) Gaffney, H. D. *Coord. Chem. Rev.* **1990**, *104*, 113.
(34) Danielson, E.; Lumpkin, R. S.; Meyer, T. J. *J. Phys. Chem.* **1987**, *91*, 1305.
(35) Adelt, M.; Devenney, M.; Meyer, T. J.; Thompson, D. W.; Treadway, J. A. *Inorg. Chem.* **1998**, *37*, 2756.

stable toward extended redox cycling through Ru^{VI}. Film stabilization may be a consequence of the large amplitude displacement required to open a bpy ring, which is inhibited in rigid or semirigid environments.[35] The same effect stabilizes poly-*cis*-$[Ru(vbpy)_2(py)_2](PF_6)_2$ toward photochemical py loss.

The film environment also affects both the thermodynamics and kinetics of electron transfer. For the $Ru^{III/II}$ couple, $E_{1/2}$ is more positive in the film than in solution at all pH values. This is a medium effect arising from the difference between the interior of the film and the external solution in stabilizing Ru^{III} relative to Ru^{II}. There is also a decrease in the sensitivity of $E_{1/2}$ to pH in the films. This is presumably a consequence of the fact that the buffer components in the solution are not readily available in the interior of the film.

Oxidation past Ru^{III} is further complicated by the requirements for proton loss and metal-oxo formation. Direct oxidation of *cis*-$[Ru^{III}(bpy)_2(py)(OH)]^{2+}$ to *cis*-$[Ru^{IV}(bpy)_2(py)(OH)]^{3+}$ is not observed in solution to +1.4 V at pH 1. The mechanism of Ru^{III} oxidation to Ru^{IV} in solution is dominated by an indirect pathway involving initial disproportionation

$$2(cis\text{-}[Ru^{III}(bpy)_2(py)(OH)]^{2+}) \rightarrow cis\text{-}[Ru^{IV}(bpy)_2(py)(O)]^{2+} + cis\text{-}[Ru^{II}(bpy)_2(py)(OH_2)]^{2+}$$

followed by oxidation of $Ru^{II}-OH_2^{2+}$ to $Ru^{III}-OH^{2+}$.[36] The disproportionation reaction proceeds by proton-coupled electron transfer as evidenced by a k_{H_2O}/k_{D_2O} kinetic isotope effect of 16. This mechanism requires close contact between $Ru-OH^{2+}$ groups for proton tunneling to occur. The utilization of this pathway must be greatly limited in the films where translational and reorientational motions are hindered. It is this effect that probably accounts for the limited accessibility to oxidation states past Ru^{III} in the films with only a small fraction of sites having the required orientation between adjacent pairs in the film environment.

In films of poly-*cis*-$[Ru(vbpy)_2(py)_2](PF_6)_2$, peak currents for the $Ru^{III/II}$ couple decrease by ~50% upon changing solvents from CH_3CN to H_2O while $E_{1/2}$ remains essentially the same. The apparent loss in electroactivity may be due to the formation of phase domains within the films with electroactive and inactive sites. Solvent effects are even more dramatic in poly-*cis*-$[Ru(vbpy)_2(OH_2)_2]^{2+}$. There is almost no evidence for couples beyond $Ru^{III/II}$ in films prepared by method I (reduction of both vbpy ligands). The higher oxidation states can be accessed, but only in small amounts, the evidence being the appearance of electrocatalytic activity with added alcohols.

In acetonitrile or dichloromethane, the films are relatively redox-active. The electroactivity is preserved through the photolysis and photoaquation steps as evidenced by the presence of higher oxidation state couples in first-scan cyclic voltammograms. Peak currents decrease with sequential oxidation−reduction scan cycles in water. Subsequent redox cycles in water must induce changes in internal film structure which greatly inhibit the proton-coupled electron-transfer steps required for access to higher oxidation states. They also decrease the peak currents for the $Ru^{III/II}$ couple.

In organic solvents, the films presumably swell, leading to an open internal structure, allowing access to counterions, protons, and water. In aqueous solution, water is apparently excluded from the films, and this inhibits internal counterion and proton transport. The "internal phase change" between the open and closed structures is reversible, at least in part. Related phenomena have been reported for polypyridyl aqua complexes in thin films of poly-4-vinylpyridine,[37] chloro-sulfonated polystyrene,[38] and Nafion.[39]

Oxidation Catalysis. In oxidative scans of poly-*cis*-$[Ru(vbpy)_2(OH_2)_2](ClO_4)_2$ in the presence of 0.1 M methanol, ethanol, or 2-propanol there is little evidence for oxidation at 50 mV/s with only slight increases observed on the anodic side of the $Ru^{III/II}$ couple compared to background currents. For *n*-butanol and benzyl alcohol, catalytic waves appear with an onset at +1.15 V for *n*-butanol and at +1.00 V for benzyl alcohol. This is the potential region for the *cis*-$[Ru^{V}(bpy)_2(OH)(O)]^{2+}$/*cis*-$[Ru^{IV}(bpy)_2(OH_2)(O)]^{2+}$ couple in solution at pH 1.

The relative reactivity of a series of alcohols determined from the magnitude of catalytic currents in controlled-potential electrolysis experiments under comparable conditions is $CH_3OH < CH_3CH_2OH < (CH_3)_2CHOH < CH_3(CH_2)_3OH < C_6H_5CH_2OH$. This order parallels the order of irreversible oxidative peak potentials for the oxidation of the alcohol at a Pt electrode in CH_3CN where the variation is from $E_{p,a} = +2.4$ V versus SCE (methanol) to $E_{p,a} = +1.60$ V (benzyl alcohol).[40]

Given the evidence for slow electron transfer and the kinetic inhibition to higher oxidation states, catalytic alcohol oxidation is presumably carried by a small fraction of sites. These may be sites which lie near the electrode surface or near channels or defects in the films which are open to proton and counterion transport and which have adjacent sites appropriately juxtaposed.

More insight into catalytic alcohol oxidation was gained from rotating disk voltammetry experiments. Oxidation of benzyl alcohol at poly-*cis*-$[Ru(vbpy)_2(OH_2)_2](ClO_4)_2$ occurs with features at +0.86 V and + 1.03 V, potentials which correspond to the $Ru^{IV/III}$ and $Ru^{V/IV}$ couples of *cis*-$[Ru(bpy)_2(OH_2)_2]^{2+}$. A small feature is observed at +1.2 V which corresponds to the $[Ru^{VI}(bpy)_2(O)_2]^{2+}/[Ru^{V}(bpy)_2(OH)(O)]^{2+}$ couple. These features are the result of reoxidation of different amounts of Ru^{III}, Ru^{IV}, and Ru^{V}, indicating reaction of benzyl alcohol with these higher states of Ru. Presumably, by the time the potential is high enough to reach Ru^{VI}, the benzyl alcohol near the electrode surface is essentially completely oxidized. These results provide clear evidence for the accessibility of the higher oxidation states within the films, even under conditions where the underlying oxidation waves are not discernible by cyclic voltammetry. Following controlled potential electrolysis, extraction of the oxidation products into dichloromethane and analysis by GC-MS identified benzaldehyde as the oxidation product with no evidence for benzoic acid.

In potential step-injection electrolysis experiments with 2-propanol as the reductant and a potential step to +1.25 V, a sustained catalytic current density of 12 μA cm^{-2} was obtained over periods as long as 1 h. The oxidation mechanism involves diffusion of the alcohol to the film−solution interface, transfer across the film−solution interface, diffusion within the film, and oxidation.[12]

The absence of a rotation rate dependence from 200 to 2500 rpm in the rotating disk experiments indicates that diffusion is not rate-limiting, at least for benzyl alcohol at 0.1 M. Assuming that solution-to-film transfer and diffusion within the film are facile, the generalized reaction scheme becomes

(36) Binstead, R. A.; Meyer, T. J. *J. Am. Chem. Soc.* **1987**, *109*, 3287.
(37) Samuels, G. J.; Meyer, T. J. *J. Am. Chem. Soc.* **1981**, *103*, 307.
(38) Surridge, N. A.; McClanahan, S. F.; Hupp, J. T.; Danielson, E.; Gould, S.; Meyer, T. J. *Inorg. Chem.* **1989**, *28*, 294.
(39) Vining, W. J.; Meyer, T. J. *J. Electroanal. Chem.* **1987**, *237*, 191.
(40) Ross, S. D.; Finkelstein, M.; Rudd, E. J. *Anodic Oxidation*, 1st ed.; Academic Press: New York, 1975; Vol. 32.

$$RR'CHOH \overset{K_p}{\rightleftharpoons} RR'CHOH_f \quad (6)$$

$$Ru_{ox} + RR'CHOH_f \overset{K_A}{\rightleftharpoons} Ru_{ox},RR'CHOH_f \quad (7)$$

$$Ru_{ox},RR'CHOH_f \xrightarrow{k} Ru_{red} + RR'C{=}O \quad (8)$$

$$Ru_{red} \xrightarrow{\text{fast}} Ru_{ox} + ne^- \quad (9)$$

K_p is the partition constant for alcohol RR′CHOH between the solution and film, $RR'CHOH_f$ is the alcohol in the film, and K_A is the association constant between the alcohol and the catalytic site in the film. Catalysis is observed for both the $Ru^{IV/III}$ and the $Ru^{V/IV}$ couples and the nature of the oxidized, Ru_{ox}, and reduced, Ru_{red}, forms depends on the applied potential.

In this kinetic limit, the catalytic current density is dictated by the rate of reoxidation of Ru_{red} to Ru_{ox}. The oxidation is carried out by the fraction of sites that are electrochemically active, f (eq 10).[41]

$$\frac{d[Ru_{red}]}{dt} \propto \frac{j_{cat}}{nFd} = fkK_AK_p[Ru_{ox}][RR'CHOH] \quad (10)$$

In this equation, n is the number of electrons transferred, F the Faraday constant, and d the film thickness. For the specific case of 2-propanol with $E_{app} = +1.3$ V and participation by Ru^{IV}, Ru^{V}, and Ru^{VI}, eq 10 becomes

$$j_{cat} = (nFdK_p)(f_{IV}k_{IV}K_{A,IV} + f_Vk_VK_{A,V} + f_{VI}k_{VI}K_{A,VI})[Ru_{ox}][(CH_3)_2CHOH] \quad (11)$$

with the f, k, and K_A values referring to each of the oxidizing sites and $[Ru_{ox}]$ is the total concentration of oxidized sites.

Equation 11 correctly predicts the linear dependence of j_{cat} on $[(CH_3)_2CHOH]$ in Figure 4.

The surface coverage results (Figure S1 in the Supporting Information) show that the catalytic current increases with Γ (and film thickness), but at the cost of a decreasing fraction of catalytically active sites. Presumably, as the film thickness is increased, a larger fraction of the active redox sites are further from the electrode and inhibited in their reoxidation.

(41) The derivation of eq 10 is in the Supporting Information.

The rotating disk voltammetry experiments reveal that, with benzyl alcohol, the oxidation chemistry is carried out mainly by Ru^{IV} and Ru^{V}. In principle, there could be different products with Ru^{IV}, Ru^{V}, and Ru^{VI} as oxidants. Ru^{VI}, the most potent of the three oxidants, may play a more important role for less reactive reductants.

Conclusions

A novel method for photofabrication of catalytically active polymer-modified electrodes has been presented. The electrochemical and photochemical preparation of the catalyst allows control over both the chemical composition of the film and the polymerization conditions dictate the ultimate electrochemical activity of the catalysts in the film matrix. This activity may be further controlled by the choice of external solvent and pH.

Experiments involving the electrocatalytic oxidation of ROH and ArOH by poly-*cis*-$[Ru^{VI}(vbpy)_2(O)_2]^{2+}$ have demonstrated the capability of these films as oxidation catalysts which retain their solution reactivity upon incorporation into a polymer-modified electrode system. The film matrix serves as a rigid environment in which the *cis*-dioxo Ru(VI) catalyst does not decompose as in solution, but where the hydrophobic and rigid nature of the film also limits accessibility to the catalytically active higher oxidation states. Bulk oxidation experiments over long times indicate that these limits may be overcome with improvements in the polymerization and film structure. With films which carry out sustained catalytic oxidation, the unique properties of the film environment may lead to materials which can, for example, perform selective oxidations, act as sensors, and serve as part of microfabricated electrocatalytic arrays.

Acknowledgment. This work was supported by the U. S. Army Research Office under Grant DAAH04-95-0144 and by the National Science Foundation under Grant CHE-9503738.

Supporting Information Available: Derivation of eq 10 and Figure S1 showing the variation of catalytic current for the oxidation of 2-propanol as a function of film thickness. This material is available free of charge via the Internet at http://pubs.acs.org.

IC990235F